JOURNAL OF CHEMICAL & ENGINEERING DATA

ARTICLE

pubs.acs.org/jced

Potentiometric, Theoretical, and Thermodynamic Studies on Equilibrium Constants of Aurintricarboxylic Acid and Determination of Stability Constants of Its Complexes with Cu^{2+}, Ni^{2+}, Zn^{2+}, Co^{2+}, Hg^{2+}, and Pb^{2+} Metal Ions in Aqueous Solution

Hasan Atabey* and Hayati Sari

Science and Arts Faculty, Chemistry Department, Gaziosmanpaşa University, 60250, Tokat, Turkey

ABSTRACT: In this study, the dissociation constants of aurintricarboxylic acid (5,5′-((3-carboxy-4-oxocyclohexa-2,5-dienylidene)-methylene)bis(2-hydroxybenzoic acid)) (ATA) together with the stability constants of its Cu^{2+}, Ni^{2+}, Zn^{2+}, Co^{2+}, Hg^{2+}, and Pb^{2+} complexes were studied potentiometrically/theoretically and determined via the SUPERQUAD computer program in aqueous media and at the ionic background of 0.1 mol·dm^{-3} of NaCl. Moreover, its thermodynamic parameters were determined in different temperatures (298 K, 308 K, and 318 K). It has been perceived that the ATA has five dissociation constants, so for LH_5 they are 2.95 (3), 3.04 (4), 3.98 (3), 9.56 (1), and 10.06 (5), respectively. The overall stability constants of its metal complexes were calculated and various formed complexes formulated as M_2L, M_2HL, M_2H_2L, M_2H_3L, and M_2H_4L between the ATA with Cu^{2+}, Ni^{2+}, Zn^{2+}, Co^{2+}, Hg^{2+}, and Pb^{2+} ions.

INTRODUCTION

Aurintricarboxylic acid (5,5′-((3-carboxy-4-oxocyclohexa-2,5-dienylidene)methylene)bis(2-hydroxybenzoic acid)) (ATA) (Figure 1) is a very important compound because of its use in a wide number of fields. Actually, biological activity[1−7] and anti-HIV activity[8−11] of ATA were researched in many studies. ATA has been shown to inhibit the replication of viruses from several different families, including human immunodeficiency virus, vesicular stomatitis virus, and the coronavirus causing severe acute respiratory syndrome.[12] In addition, ATA has antiviral features against some viruses, such as SARS-CoV and other pathogenic positive-strand RNA viruses,[13,14] group-1 and group-2 influenza viruses,[15] and Enterovirus 71 (EV71).[16]

ATA has been used as an antiapoptotic drug to counteract ischemic or cytotoxic injury to neurons.[17] Additionally, ATA is well-known as an endonuclease inhibitor.[18,19]

Fluorescence spectra and fluorescence quantum yield of ATA were studied for the first time. It was found that ATA solutions with pH 3 similar to 12 produced fluorescence when irradiated with ultraviolet rays. The maximum excitation wavelength and the maximum emission wavelength are 297 nm and 409 run, respectively.[20] Resonance light scattering (RLS) and absorption and fluorescence spectra of ATA were studied. In solutions with pH 3.7 to pH 11.0, the RLS signal was very weak but increased sharply with a decrease in pH when pH < 3.7 and reached a maximum at pH 2.7.[21]

Finally, many studies have been done related to ATA. However, its acid−base properties and complexation tendency have not been explained enough. The dissociation of ATA plays an important role in the complexation and its biological activity. Therefore, the accurate determination of dissociation and stability constant values is very important for explaining the antioxidant behavior of ATA and interaction with metal ions. Consequently, in the present study, dissociation constants of ATA and stability constants of its complexes with Cu^{2+}, Ni^{2+}, Zn^{2+}, Co^{2+}, Hg^{2+}, and Pb^{2+} ions were determined using the potentiometric titration method which is accepted as a powerful and simple electroanalytical technique for determination of stability constants.[22−24] The potentiometric studies were carried out at the metal:ATA molar ratios of 2:1, and each titration was repeated in several series of independent measurements.

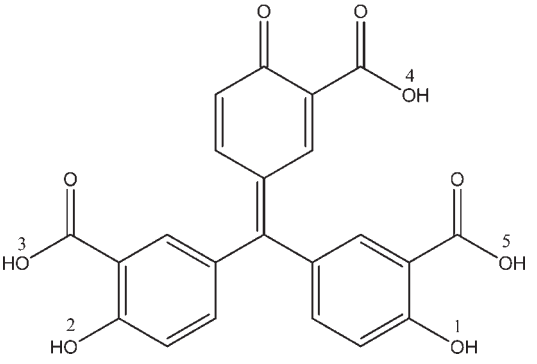

Figure 1. Chemical structure of ATA.

EXPERIMENTAL SECTION

Apparatus and Materials. All the transition metal salts and NaCl used in this research were purchased from Merck, potassium hydrogen phthalate (KHP) from Fluka, and ATA (analytical grade), 0.1 mol·dm^{-3} NaOH, and 0.1 mol·dm^{-3} HCl as standard from Aldrich. All reagents were of analytical

Received: May 31, 2011
Accepted: September 9, 2011
Published: September 28, 2011

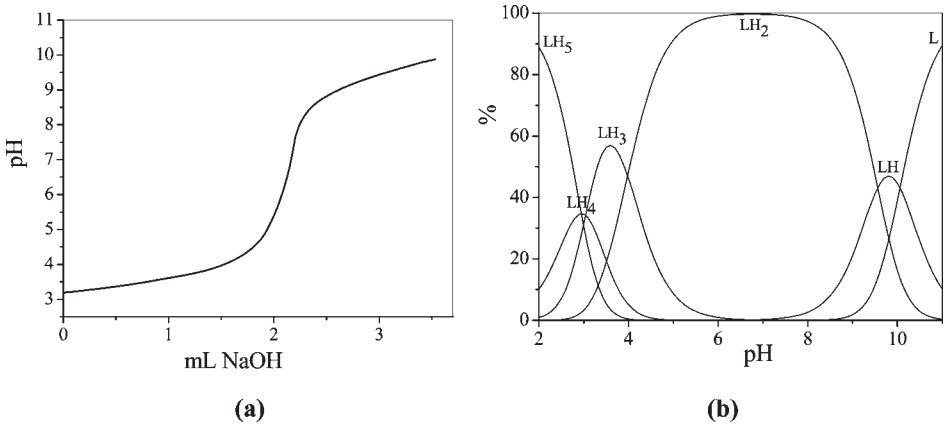

Figure 2. (a) Titration curve for ATA and (b) the species distribution curves of ATA (298 K, I = 0.1 mol·dm^{-3} NaCl, 0.05 mmol of HCl).

quality and were used without further purification. Solutions of metals ions (2.10^{-3} mol·dm^{-3}) were prepared from $CuCl_2$, $ZnCl_2$, $NiCl_2$, $CoCl_2$, $HgCl_2$, and $PbCl_2$ as received and standardized with ethylenediaminetetraacetic acid (EDTA).[25]

Potassium hydrogen phthalate (0.05 M, KHP) was prepared for calibration of electrode systems. ATA ($2\cdot10^{-3}$ mol·dm^{-3}) in water, 0.025·mol dm^{-3} NaOH, and 0.1 mol·dm^{-3} HCl were prepared. NaOH concentration (0.025 mol·dm^{-3}) was standardized with primer standard KHP solution by pH-metric titration. The solutions were purged with nitrogen (99.9 %) through the cell solutions. NaCl stock solution (1.0 mol·dm^{-3}) was prepared.

For the solutions, CO_2-free double-distilled deionized water was obtained with an aquaMAX-*Ultra* water purification system (Young Lin Inst.). Its resistivity was 18.2 MΩ·cm^{-1}. pH-metric titrations were performed using the Molspin pH meter with an Orion 8102BNUWP ROSS ultra combination pH electrode. The temperature in the double-wall glass titration vessel was constantly controlled using a thermostat (DİGİTERM 100, SELECTA). The cell solution was stirred during the titration at constant speed. The electrode was calibrated according to instructions of the Molspin Manuel.[26]An automatic buret was connected to the Molspin pH-mV-meter. The pH electrode was calibrated with buffer solution (KHP) of pH 4.005, 4.018, and 4.038 at 298 K, 308 K, and 318 K, respectively.[27] The SUPERQUAD computer program was used for the calculation of both protonation and stability constants.[28]

Potentiometric Measurements. All potentiometric pH measurements were made on solutions in a 100 mL double-walled glass vessel using an Orion 8102BNUWP ROSS ultra combination pH electrode, and the temperature was controlled by circulating water through the double-walled glass vessel, from a constant-temperature bath (DIGITERM 100, SELECTA). The cell was equipped with a magnetic stirrer. Atmospheric CO_2 was excluded from the titration cell with a purging steam of purified N_2. The system was maintained at an ionic strength of 0.1 mol·dm^{-3} by NaCl as a supporting electrolyte. In experiment, a solution containing about 0.01 mmol of ATA was placed in the cell. The required amounts of 1.0 mol·dm^{-3} NaCl and 0.1 mol·dm^{-3} HCl were added. Finally, doubly distilled deionized water was added to the cell to a total volume of 50 mL, and titration was started. The pH data points were collected after each addition of 0.03 cm^3 of the standardized NaOH solution. The second solution contains the same amounts of component plus about 0.02 mmol of each metal ion for the three times.

Table 1. Dissociation Constants of ATA in the Study and Literature (298 K, I = 0.1 mol·dm^{-3} NaCl, 0.05 mmol of HCl)

ligand	species	$\log_{10}\beta$	pK_a (this work)	pK_a (literature)
ATA	LH_5	10.06 (2)	2.95 (2)	
	LH_4	19.62 (1)	3.04 (4)	
	LH_3	23.60 (2)	3.98 (3)	
	LH_2	26.64 (4)	9.56 (1)	8.63[29] to 8.93[30]
	LH	29.59 (6)	10.06 (5)	8.85[29] to 9.76[30]

All titrations have been carried out between pH 3.0 and 11.0 and under a nitrogen atmosphere.

RESULTS AND DISCUSSION

Dissociation Constants. Dissociation constants were potentiometrically calculated from a series of several independent measurements. The titration curve and the species distribution curves for ATA in water with NaOH as a titrant are shown in Figure 2.

If LH_n (n = 5) denotes the fully protonated form of the ATA, general notation of its protonation equilibra is as follows

$$LH_n + H_2O \rightleftharpoons LH_{n-1} + H_3O^+ \quad (1)$$

In each stage, one proton dissociates, and dissociation constants (K_n; n = 1−5) are given as

$$K_n = \frac{[LH_{n-1}]\cdot[H_3O]}{[LH_n]} \quad (2)$$

Five pK_a values are obtained from this ligand: three of them are associated with the carboxyl oxigen atoms, and the other two are associated with hydroxyl groups. These pK_a values of ATA were calculated with very low standard deviation (Sigma value (δ): 0.70)[28] and determined as 2.95 (3), 3.04 (4), 3.98 (3), 9.56 (1), and 10.06 (5), respectively. A comparison the pK_a values of the ATA is given in Table 1.

According to Table 1, there are five acidic centers in ATA. These acidic centers are three carboxyl groups and two hydroxyl groups. In the literature, the stepwise protonation constants of the ligand and formation constants of the chelate have been determined using the Calvin−Bjerrum technique,[30] and two pK_a values (two hydroxyl groups) were reported because aurintricarboxylate salt was used as ligand and different ionic strength

dx.doi.org/10.1021/je200528f |J. Chem. Eng. Data 2011, 56, 3866–3872

Table 2. Calculated H_f, TE, and PA Values with the AM1 Method for ATA and Its Monoprotonated Forms

species	TE (kcal·mol^{-1})	H_f	PA
ATA	−135805.72	−200.16	-
1O−H_2^+	−136031.36	−110.91	277.95
2O−H_2^+	−136074.20	−97.13	264.17
3O−H_2^+	−136014.98	−94.49	261.53
4O−H_2^+	−136006.42	−85.97	253.01
5O−H_2^+	−136015.81	−95.36	262.40

(I = 0.02 mol·dm^{-3} by NaOCl) was used in the studies.[29,30] However, although ionic strength is different, pK_{a4} and pK_{a5} values were still shown similar to the literature.

All ligand species of ATA, which are expected to be formed under our experimental conditions, are presented in the distribution diagrams illustrated in Figure 2. The ligand species, which occurred in solution under our experimental conditions, are LH_5, LH_4, LH_3, LH_2, and LH. The experimental parameters and conditions used here are the same as those used to determine the stability constants. The distribution diagram of the ligand assists the determination of the experimental conditions where the coordination with metal ions would take place, especially in terms of pH.

Theoretical Calculation. Semiempiric molecular orbital (SEMO) methods are one of the theoretical calculations that will assist in comprehending the protonation sequence of phenolate and carboxylate groups in the ligand molecule. The method is very useful for determination of the order of protonation in polyprotic coordination molecules.[31−34] The formation heats (H_f) and the total energies (TE) of the ligands and monoprotonated species were calculated by the Semi-Empirical AM1 method. In addition, the proton affinity (PA) of each oxygen atom in the ligands was found using formation heats in the following equation and given in Table 2.

$$PA = 367.2 + \Delta H_f^\circ(B) - \Delta H_f^\circ(BH^+) \quad (3)$$

where PA is the proton affinity of B types; $\Delta H_f^\circ(B)$ is the formation heat of the B molecule; $\Delta H_f^\circ(BH^+)$ is the formation heat of the BH^+ molecule; and 367.2 is the formation heat of H^+.[35]

Proton affinity gives information about protonation order. Since the oxygen atom having the highest PA is 1O in ATA, the first protonated oxygen is 1O in this ligand. According to the calculated results (TE, H_f, and PA), protonation orders of oxygen atoms in the ATA are 1O, 2O, 5O, 3O, and 4O. The reason for 1O being the first protonated oxygen in the ATA is the inductive effect of the hydrogen bond with the carbonyl oxygen. In conclusion, according to the data obtained from theoretical calculation, 10.06 (pK_{a5}), 9.56 (pK_{a4}), 3.98 (pK_{a3}), 3.04 (pK_{a2}), and 2.95 (pK_{a1}) values belong to 1O, 2O, 5O, 3O, and 4O in ATA, respectively.

As a result of theoretical and experimental calculations, ATA has three acidic carboxyl groups and two ionizable hydroxy groups, and the enhancement of carboxylic acidity is due to the inductive effect of the neighboring hydroxy group. This is essential in complying with the technical report of IUPAC[36] about the proton and metal ion stability constants of the *ortho*-hydroxy-carboxylic acid complexes. Clearly, due to intramolecular hydrogen bonding between the neighboring −OH and −COOH groups and the basic nature of the −OH group, the protonation of the phenolate group takes place at a very high pH level. Because of this ortho-effect, the protonation constant of the phenolate group of various aromatic *ortho*-hydroxycarboxylic acids is significantly higher than that of phenol, and the protonation constant of the carboxylate group is significantly smaller than that of benzoic acid.[37]

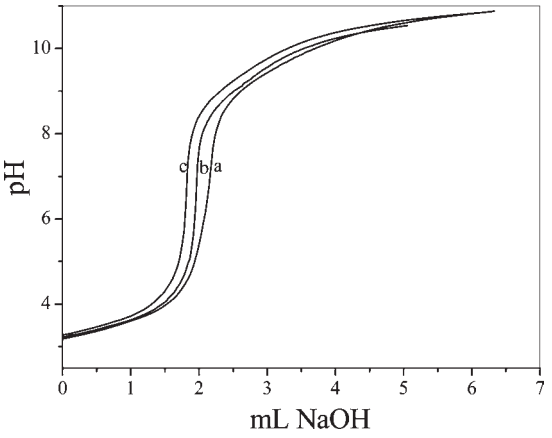

Figure 3. Titration curve for ATA in different temperatures: (a) 298 K, (b) 308 K, (c) 318 K (I = 0.1 mol·dm^{-3} NaCl, 0.05 mmol of HCl).

Table 3. pK_a Values of ATA in Different Temperatures (298 K, I = 0.1 mol·dm^{-3} NaCl, 0.05 mmol of HCl)

Temperatures T/K					
298		308		318	
$\log_{10}\beta$	pK_a	$\log_{10}\beta$	pK_a	$\log_{10}\beta$	pK_a
10.06 (2)	2.95 (3)	10.31 (3)	2.83 (1)	10.49 (7)	2.78 (3)
19.62 (1)	3.04 (4)	19.64 (3)	3.24 (2)	19.73 (6)	3.25 (6)
23.60 (2)	3.98 (3)	23.28 (4)	3.64 (2)	23.35 (2)	3.62 (1)
26.64 (4)	9.56 (1)	26.51 (2)	9.33 (3)	25.59 (1)	9.24 (5)
29.59 (6)	10.06 (5)	29.34 (7)	10.31 (3)	29.37 (3)	10.49 (1)

Finally, it can be assumed that the coordination of ATA with the metal ion occurs via the carboxylic group and the hydroxyl group to form complexes. Intra-hydrogen bonding between the hydrogen of the carboxylic group and the oxygen of the hydroxy group is expected to take place within the ligand molecule in the solution, but it is not expected that such bonding will cause significant obstruction to the coordination of the ligand to the metal ion.[38]

Thermodynamic Study. Titration curves for ATA in different temperatures and the dissociation constants of ATA have been evaluated at 298 K, 308 K, and 318 K and are given in Figure 3 and Table 3.

Figure 3 represents the titration curves for different temperatures (298 K, 308 K, and 318 K, respectively). Comparing the titration curves of the ATA (Figure 3) in different temperatures shows that lower pH in high temperature. This can simply be explained as a result of proton release from the ligand.[38] The amount of protons released depends on the strength of the intermolecular hydrogen bond. In other words, it can be said that when temperatures are increased the strength of the intermolecular hydrogen bonds is decreased.

The slope of the plot pK^H or $\log_{10} K$ vs $1/T$ was utilized to evaluate the enthalpy change ΔH for the dissociation process,

Table 4. Thermodynamic Functions of ATA (298 K, I = 0.1 mol·dm^{-3} NaCl, 0.05 mmol of HCl)

		Gibbs energy	enthalpy	entropy
	dissociation constants	kJ·mol^{-1}	kJ·mol^{-1}	J·mol^{-1}·K^{-1}
T/K	pK_{a1} values	ΔG	ΔH	ΔS
298	2.95	33.69		−336.24
308	2.83	32.74	−66.51	−327.57
318	2.78	32.77		−322.34
T/K	pK_{a2} values	ΔG	ΔH	ΔS
298	3.04	34.68		162.63
308	3.24	37.53	83.14	150.54
318	3.25	38.40		145.25
T/K	pK_{a3} values	ΔG	ΔH	ΔS
298	3.98	45.33		−598.51
308	3.64	42.31	−133.02	−578.67
318	3.62	42.76		−570.71
T/K	pK_{a4} values	ΔG	ΔH	ΔS
298	9.56	109.01		−784.28
308	9.33	108.32	−124.71	−769.06
318	9.24	108.82		−758.22
T/K	pK_{a5} values	ΔG	ΔH	ΔS
298	10.06	114.70		173.08
308	10.31	119.65	166.28	153.89
318	10.49	123.67		138.33

respectively. From the Gibbs energy change, ΔG and ΔH values can deduce the entropy changes ΔS using the well-known relationships eq 4 and 5

$$\Delta G = -2.303RT \log_{10} K \quad (4)$$

$$\Delta S = (\Delta H - \Delta G)/T \quad (5)$$

All thermodynamic parameters of the dissociation process of ATA are recorded in Table 4.

Some conclusions can be drawn from the above results: the pK^{H} values decrease with increasing temperature (see pK_{a1}, pK_{a3}, and pK_{a4}), and the acidity of the ligands increases, independently of the nature of the substituent.[39] A positive value of ΔH indicates that the process is endothermic (see pK_{a2} and pK_{a5}). A large positive value of ΔG indicates that the dissociation process is not spontaneous.[40]

This case can be shown between pK_{a1}, pK_{a2}, pK_{a3} values and pK_{a4}, pK_{a5} values. The dissociation processes for LH, LH_2, and LH_3 have negative values of ΔS due to increased order as a result of the salvation processes.

Stability Constants. The ligand behaves as a tetradentate ligand, and the carboxyl and the *ortho*-hydroxy groups of the ligand coordinate to the metal ions. Diverse metal complexes were produced in the solution under the experimental conditions for each metal ion used. The species distribution curves of a variety of complexes formed in the solution were calculated and reviewed by the SUPERQUAD computer program.

The cumulative stability constants (β_{mlh}) are defined by eqs 6 and 7.

$$mM + lL + hH \rightleftharpoons M_mL_lH_h \quad (6)$$

$$\beta_{mlh} = \frac{[M_mL_lH_h]}{[M]^m[L]^l[H]^h} \quad (7)$$

where M is the Cu^{2+} ion, L is ligand, and H is proton and m, l, and h are the respective stoichiometric coefficients. Potentiometric titration of complex systems of respective metal ions including Cu^{2+}, Ni^{2+}, Zn^{2+}, Co^{2+}, Hg^{2+}, and Pb^{2+} with ATA in aqueous solution were carried out to evaluate the stoichiometry and stability of various species. The complexes formulated as M_2L, M_2LH, M_2LH_2, M_2LH_3, and M_2LH_4 between the ATA and the Cu^{2+}, Ni^{2+}, Zn^{2+}, Co^{2+}, Hg^{2+}, and Pb^{2+} ions are depending on pH. In other words, the pH function regulates the subsistence of plausible species in solution.[41] Respectively, the obtained overall stability constants of these species are given in Table 5.

ATA occurs in three aromatic moieties. Two of these moieties are α-hydroxycarboxylic acid systems. The hydroxycarboxylic acids contain two donor groups, the hydroxyl and the carboxylate groups (bidentate), and therefore they are all potentially tetradentate ligands.

Another moiety is α-oxo-carboxylic acid, which contains only one donor group, carboxylate (monodentate), and therefore it cannot attempt complexation with metal ions. So, chemical structures for M_2−ATA[42] complex systems can be given as in Figure 4.

Generally, the complexes which have been traced in solution are M_2L, M_2LH, M_2LH_2, M_2LH_3, and M_2LH_4, where LH_5 represents the neutral ligand; other species with H less than 5 are the deprotonated species of the (ATA) ligand; and M represents one of the following metal ions Cu^{2+}, Ni^{2+}, Zn^{2+}, Co^{2+}, Hg^{2+}, and Pb^{2+}, bearing in mind that not all the metal ions are capable of forming all the above complex species.

The species distribution diagrams of the Cu^{2+}−ATA system are shown in Figure 5. Cu_2L−Cu_2H_4L complexes were obtained in the solution under experimental conditions between pH 3 and 11. At about the pH of 3, approximately 95 % of the total Cu^{2+} turns to Cu_2H_4L, forming the main constituent of the complex species. Cu_2H_3L formed about 75 % of the total Cu^{2+}, which revealed its maximum occurrence at a pH of about 5. The maximum occurrence of Cu_2H_2L (about 85 %) was at a pH of about 7, while the maximum occurrence of Cu_2HL (about 60 %) was at a pH of about 9. In more basic solution and at a pH just above 9, another species Cu_2L starts to develop and reaches its maximum occurrence in the solution, at a pH of about 11 (forming nearly 98 % of the total Cu^{2+}).

In the Ni^{2+}−ATA system (see Figure 6), Ni_2H_4L−Ni_2L complexes were obtained in the solution between pH 3 and 11. Three main complexes were seen in the Ni^{2+}−ATA system according to Figure 7. While two of these complexes formed (Ni_2H_4L−Ni_2H_3L) take place in the acidic region, the Ni_2L complex formed takes place in the basic region (nearly 98 % of the total Ni^{2+} at pH 11). Ni_2H_2L formed about 55 % of the total Ni^{2+}, which revealed its maximum occurrence at a pH of about 8.3, while the maximum occurrence of Ni_2HL (less than about 40 %) was at a pH of about 9.

Figure 7 demonstrates the species distribution diagrams for the Zn^{2+}−ATA system. Species start to exist at even lower pH values than $Ni^{2+}$and Cu^{2+}complexes. According to Figure 7,

Table 5. Overall Stability Constants in the M^{2+}—ATA System (298 K, I = 0.1 mol·dm^{-3} NaCl, 0.05 mmol of HCl)

species	Cu^{2+}	Ni^{2+}	Zn^{2+}	Co^{2+}	Hg^{2+}	Pb^{2+}
mhl	$\log_{10}\beta$					
201	20.56 (3)	19.56 (6)	19.59 (9)	20.56 (4)	20.56 (6)	20.71 (5)
211	29.81 (3)	28.49 (6)	28.31 (4)	29.56 (8)	29.56 (6)	29.29 (5)
221	37.92 (3)	37.41 (4)	36.63 (2)	38.61 (5)	38.61 (4)	38.44 (4)
231	43.86 (4)	45.34 (6)	41.24 (5)	46.65 (3)	46.65 (3)	45.71 (3)
241	48.24 (5)	50.83 (6)	-	51.79 (4)	51.79 (2)	50.55 (6)

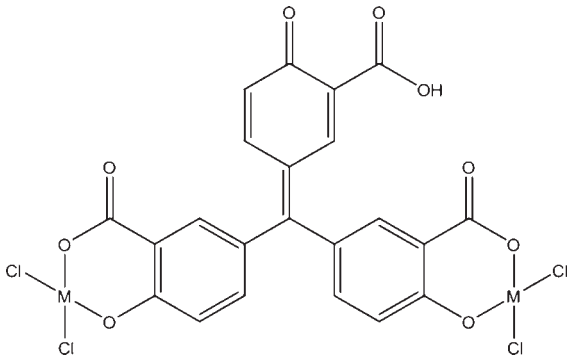

Figure 4. Chemical structures for M_2—ATA complex systems.

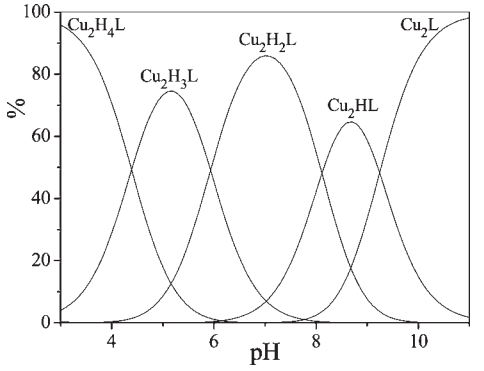

Figure 5. Species distribution curves for ATA with Cu^{2+} complexes (298 K, I = 0.1 mol·dm^{-3} NaCl, 0.05 mmol of HCl).

three main complexes were obtained in the Zn^{2+}—ATA system. One of the species (Zn_2H_3L) existed in the acidic region (about pH 3.5), while Zn_2H_3L formed about 95 % of the total Zn^{2+} and took place in the neutral region (about pH 7) and Zn_2L formed about 99 % of the total Zn^{2+}, which revealed its maximum occurrence at a pH of about 11. Another species (Zn_2HL) started to occur at pH 6.5 and reached the maximum at pH 8.5, less than 50 % of the total Zn^{2+}.

Species distribution curves for Co^{2+}—ATA systems are shown in Figure 8. Co_2H_3L—Co_2L complexes were obtained between pH 3 and 11. The Co^{2+} ion is capable of forming all the possible species which might be expected as a result of coordination and dissociation processes between the ATA ligand and metal ion. Three main complexes (Co_2H_4L, Co_2H_3L, Co_2L) were obtained in solution under the experimental conditions. Co_2H_4L, Co_2H_3L, and Co_2L complexes take place in the acidic, neutral, and basic region and at about pH 3, pH 7, and pH 11 and

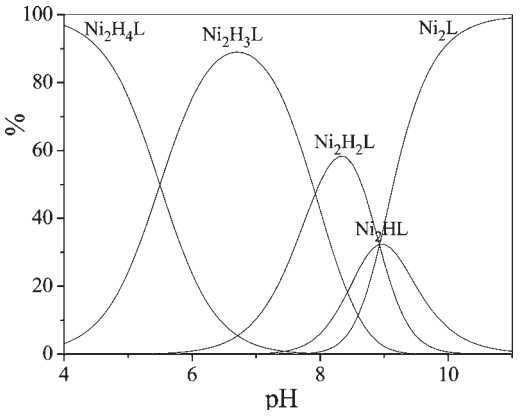

Figure 6. Species distribution curves for ATA with Ni^{2+} complexes (298 K, I = 0.1 mol·dm^{-3} NaCl, 0.05 mmol of HCl).

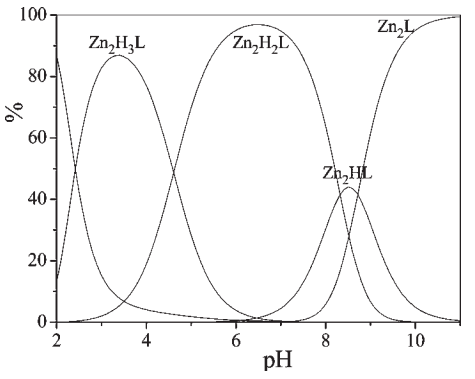

Figure 7. Species distribution curves for ATA with Zn^{2+} complexes (298 K, I = 0.1 mol·dm^{-3} NaCl, 0.05 mmol of HCl).

relatively 99 %, 95 %, and 98 % of the total Zn^{2+} solution, respectively.

The Hg^{2+}—ATA complex was considered in this study to reveal the extent of the coordination properties against toxic heavy metals (Hg, Pb) of the (ATA) ligand. A variety of species started to appear in the solution at a pH of 3. The Hg^{2+}—ATA system (see Figure 9) is quite similar to Co^{2+} and Ni^{2+} complexes. Similarity, three main complexes (Hg_2H_4L, Hg_2H_3L, Hg_2L) exist around the acidic, neutral, and basic region, respectively. The Hg_2H_3L and Hg_2H_3L species were formed in the acidic and neutral medium, and their formation span between pH just above 3 and pH just above 6 with a maximum availability of about 100 % at pH 3 for the first and of the same percentage with a pH of 7 for the second. The other species Hg_2L formed in pH 11, and its maximum availability of 99 % was in the basic area.

dx.doi.org/10.1021/je200528f |J. Chem. Eng. Data 2011, 56, 3866–3872

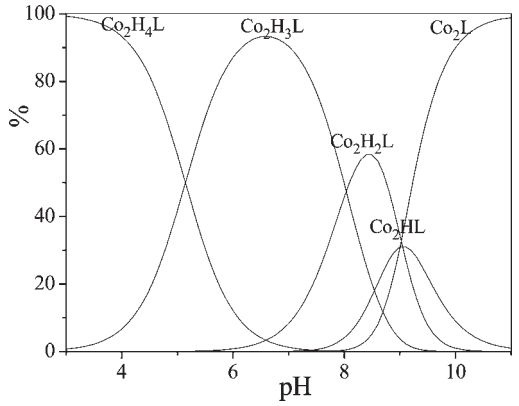

Figure 8. Species distribution curves for ATA with Co^{2+} complexes (298 K, I = 0.1 mol·dm^{-3} NaCl, 0.05 mmol of HCl).

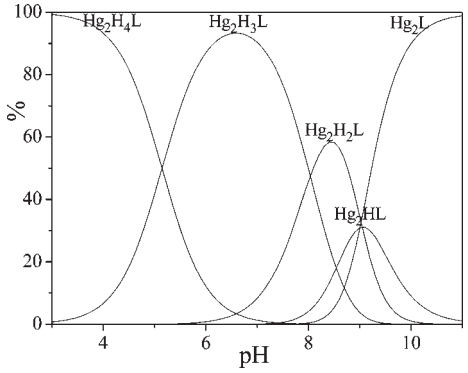

Figure 9. Species distribution curves for ATA with Hg^{2+} complexes (298 K, I = 0.1 mol·dm^{-3} NaCl, 0.05 mmol of HCl).

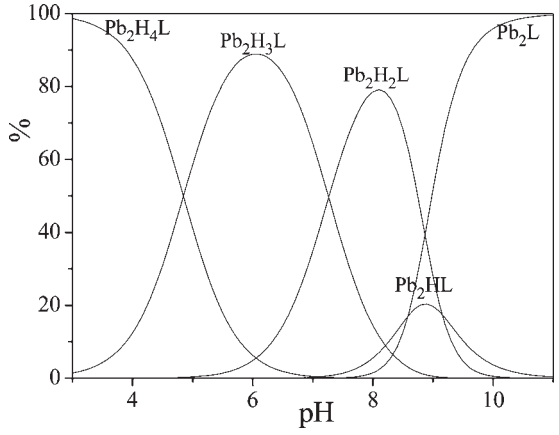

Figure 10. Species distribution curves for ATA with Pb^{2+} complexes (298 K, I = 0.1 mol·dm^{-3} NaCl, 0.05 mmol of HCl).

Pb^{2+}—ATA complexes exist in solution at different shapes as in the case of the previous metal complexes. According to Figure 10, Pb_2L—Pb_2H_4L complexes were obtained in the solution under experimental conditions between pH 3 and 11. At about the pH of 3, approximately 99 % of the total Pb^{2+} turns to Pb_2H_4L, forming the main constituent of the complex species.

Pb_2H_3L formed about 90 % of the total Pb^{2+}, which revealed its maximum occurrence at a pH of about 6. The maximum occurrence of Pb_2H_2L (about 80 %) was at a pH of about 8, while the maximum occurrence of Pb_2HL (about 20 %) was at a pH of about 9. In more basic solution and at a pH just above 10, another species Pb_2L started to develop and reached its maximum occurrence in the solution, at a pH of about 11 at relatively 98 % of the total Pb^{2+}.

As result of that mentioned above, ATA contains hydroxyl and carboxyl groups, which are ortho position to each other, and included four donor oxygen atoms which providd the coordination according to M_2L form. Complexation starts when carboxyl and hydroxyl groups that participate in the coordination are dissociated. First, carboxyl groups ionize and then hydroxyl groups. Our results show that, when both of the hydroxyl groups are ionized, the ligand (ATA) behaves as a tetradentate ligand, and the M_2L complex form occurs. Therefore, the highest ratio of the total M^{2+} turns into M_2L in all metal complexes in our experimental conditions. When one of the hydroxyl groups is ionized, the ligand (ATA) behaves as a tridentate ligand, and the M_2L complex does not happen. Therefore, the lowest ratio of the total M^{2+} turns into M_2HL in all metal complexes.

CONCLUSION

In this study, the dissociation constants of aurintricarboxylic acid (5,5′-((3-carboxy-4-oxocyclohexa-2,5-dienylidene)methylene)-bis(2-hydroxybenzoic acid)) (ATA) together with the stability constants of its Cu^{2+}, Ni^{2+}, Zn^{2+}, Co^{2+}, Hg^{2+}, and Pb^{2+} complexes were studied potentiometrically/theoretically and determined via the SUPERQUAD computer program in aqueous media and at the ionic background of 0.1 mol·dm^{-3} of NaCl. Moreover, its thermodynamic parameters were determined in different temperatures (298 K, 308 K, and 318 K). Dissociation constants of ATA were determined as pK_{a1} = 2.95 (3), pK_{a2} = 3.04 (4), pK_{a3} = 3.98 (3), pK_{a4} = 9.56 (1), and pK_{a5} = 10.06 (5). The overall stability constants of its metal complexes were calculated through computer refinement of the pH—volume data, and the results are presented Tables 1 to 5. Various formed complexes were formulated as M_2L, M_2HL, M_2H_2L, M_2H_3L, and M_2H_4L between the ATA with Cu^{2+}, Ni^{2+}, Zn^{2+}, Co^{2+}, Hg^{2+}, and Pb^{2+} ions.

AUTHOR INFORMATION

Corresponding Author

*E-mail: hasatabey@gmail.com.

Funding Sources

The author gratefully acknowledges the support of this work by the Scientific Research Council of Gaziosmanpaşa University.

REFERENCES

(1) Strehblow, C.; Sperker, W.; Hevesi, A.; Garamvolgyi, R.; Petrasi, Z.; Shirazi, M.; Sylven, C.; Weiss, T.; Lotan, C.; Pugatsch, T.; Ben-Sasson, S. A.; Orlowski, M.; Glogar, D.; Gyongyosi, M. Paradoxical effects of aurintricarboxylic acid and RG-13577: Acute thrombosis and in-stent stenosis in a passive-coated stent. *J. Endovasc. Ther.* **2006**, *13*, 94–103.

(2) Cho, H.; Lee, D. Y.; Shrestha, S.; Shim, Y. S.; Kim, K. C.; Kim, M. K.; Lee, K. H.; Won, J.; Kang, J. S. Aurintricarboxylic acid translocates across the plasma membrane, inhibits protein tyrosine phosphatase and prevents apoptosis in PC12 cells. *Mol. Cell* **2004**, *18*, 46–52.

(3) Lee, D. Y.; Kim, M. K.; Kim, M. J.; Bhattarai, B. R.; Kafle, B.; Lee, K. H.; Kang, J. S.; Cho, H. Antiapoptotic effect of aurintricarboxylic acid. Extracellular action versus inhibition of cytosolic protein tyrosine phosphatises. *Bull. Korean Chem. Soc.* **2008**, *29*, 342–346.

(4) Posner, A.; Raser, K. J.; Hajimohammadreza, I.; Yuen, P. W.; Wang, K. K. W. Aurintricarboxylic acid is an inhibitor of mu- and m-calpain. *Biochem. Mol. Biol. Int.* **1995**, *36*, 291–299.

(5) Klein, P.; Cirioni, O.; Giacometti, A.; Scalise, G. In vitro and in vivo activity of aurintricarboxylic acid preparations against cryptosporidium parvum. *J. Antimicrob. Chemother.* **2008**, *62*, 1101–1104.

(6) Kim, H. K.; Kim, J. E.; Park, C. M.; Kim, Y. T.; Han, K. S.; Cho, H. I. Aurintricarboxylic acid upregulates the thrombomodulin expression of endothelial cells and peripheral blood monocytes. *Blood Coagulation Fibrinolysis* **2008**, *19*, 489–494.

(7) Ghosh, U.; Giri, K.; Bhattacharyya, N. P. Interaction of aurintricarboxylic acid (ATA) with four nucleic acid binding proteins DNase I, RNase A, reverse transcriptase and Taq polymerase. *Spectrochim. Acta A* **2009**, *74*, 1145–1151.

(8) Cushman, M.; Wang, P. L.; Chang, S. H.; Wild, C.; Declercq, E.; Schols, D.; Goldman, M. E.; Bowen, J. A. Preparation and Anti-Hiv Activities of Aurintricarboxylic Acid Fractions and Analogs - Direct Correlation of Antiviral Potency with Molecular-Weight. *J. Med. Chem.* **1991**, *34*, 329–337.

(9) Cushman, M.; Kanamathareddy, S.; Declercq, E.; Schols, D.; Goldman, M. E.; Bowen, J. A. Synthesis and Anti-Hiv Activities Of Low-Molecular-Weight Aurintricarboxylic Acid Fragments And Related-Compounds. *J. Med. Chem.* **1991**, *34*, 337–342.

(10) Reymen, D.; Witvrouw, M.; Este, J. A.; Neyts, J.; Schols, D.; Andrei, G.; Snoeck, R.; Cushman, M.; Hejchman, E.; DeClercq, E. Mechanism of the antiviral activity of new aurintricarboxylic acid analogues. *Antiviral Chem. Chemother.* **1996**, *7*, 142–152.

(11) Zhu, H. M.; Chen, W. Z.; Wang, C. X. Molecular dynamics simulation on the complex of HIV-1 integrase and the inhibitor aurintricarboxylic acid. *Acta Chim. Sin.* **2004**, *62*, 745–749.

(12) Myskiw, C.; Deschambault, Y.; Jefferies, K.; He, R. T.; Cao, J. X. Aurintricarboxylic acid inhibits the early stage of vaccinia virus replication by targeting both cellular and viral factors. *J. Virol.* **2007**, *81*, 3027–3032.

(13) Yap, Y. L.; Zhang, X. W.; Andonov, A.; He, R. T. Structural analysis of inhibition mechanisms of Aurintricarboxylic Acid on SARS-CoV polymerase and other proteins. *Comput. Biol. Chem.* **2005**, *29*, 212–219.

(14) Walther, W.; Stein, U.; Siegel, R.; Fichtner, I.; Schlag, P. M. Use of the nuclease inhibitor aurintricarboxylic acid (ATA) for improved non-viral intratumoral in vivo gene transfer by jet-injection. *J. Gene Med.* **2005**, *7*, 477–485.

(15) Hung, H. C.; Tseng, C. P.; Yang, J. M.; Ju, Y. W.; Tseng, S. N.; Chen, Y. F.; Chao, Y. S.; Hsieh, H. P.; Shih, S. R.; Hsu, J. T. A. Aurintricarboxylic acid inhibits influenza virus neuraminidase. *Antiviral Res.* **2009**, *81*, 123–131.

(16) Hung, H. C.; Chen, T. C.; Fang, M. Y.; Yen, K. J.; Shih, S. R.; Hsu, J. T. A.; Tseng, C. P. Inhibition of enterovirus 71 replication and the viral 3D polymerase by aurintricarboxylic acid. *J. Antimicrob. Chemother.* **2010**, *65*, 676–683.

(17) Heiduschka, P.; Thanos, S. Aurintricarboxylic acid promotes survival and regeneration of axotomised retinal ganglion cells in vivo. *Neuropharmacology.* **2000**, *39*, 889–902.

(18) Beery, R.; Haimsohn, M.; Wertheim, N.; Hemi, R.; Nir, U.; Karasik, A.; Kanety, H.; Geier, A. Activation of the insulin-like growth factor 1 signaling pathway by the antiapoptotic agents aurintricarboxylic acid and Evans blue. *Endocrinology* **2001**, *142*, 3098–3107.

(19) Liang, F. B.; Huang, Z. H.; Lee, S. Y.; Liang, J.; Ivanov, M. I.; Alonso, A.; Bliska, J. B.; Lawrence, D. S.; Mustelin, T.; Zhang, Z. Y. Aurintricarboxylic acid blocks in vitro and in vivo activity of YopH, an essential virulent factor of Yersinia pestis, the agent of plague. *J. Biol. Chem.* **2003**, *278*, 41734–41741.

(20) Wei, Y. J.; Kang, Z. M.; Qi, X. J.; Zhang, Y. P.; Liu, C. G. Fluorescence spectra and fluorescence quantum yield of aurintricarboxylic acid. *Acta Chim. Sin.* **2001**, *59*, 1619–1622.

(21) Wei, Y. J.; Kang, Z. M.; Qi, X. J.; Mo, L. P.; Liu, C. G.; Zhou, Q. Z. Resonance light scattering of aurintricarboxylic acid. *Spectrosc. Spect. Anal.* **2003**, *23*, 115–118.

(22) Serjeant, E. P. *Potantiometry and Potantiometric Titrations*; Wiley: New York, 1984.

(23) Sari, H.; Covington, A. K. Determination of acid dissociation constants of 4-(2′-Benzimidazolyl)-3-thiabutanoic acid and related compounds and stability constants of their divalent metal complexes with copper, nickel, and zinc. *J. Chem. Eng. Data* **2005**, *50*, 1425–1429.

(24) Sari, H.; Covington, A. K. Dissociation constants of morpholino- and piperidino-methylphosphonic acids and stability constants of their copper, nickel, and zinc complexes. *J. Chem. Eng. Data* **2005**, *50*, 1438–1441.

(25) Jeffery, G. H.; Bassett, J.; Mendham, J.; Denney, R. C. *Vogel's Textbook of Quantitative Chemical Analysis*, 5th ed.; Longman: London, 1989.

(26) Pettit, L. D. *Academic Software*; Sourby Farm: Timble, Otley, LS21 2PW, UK, 1992.

(27) IUPAC Recommendations. Measurement of pH Definition, Standards, and Procedures. *Pure Appl. Chem.* **2002**, *74* (11), 2169–2200.

(28) Gans, P.; Sabatini, A.; Vacca, A. SUPERQUAD: an improved general program for computation of formation constants from potentiometric data. *J. Chem. Soc., Dalton Trans.* **1985**, *6*, 1195–1200.

(29) Banerjee, A.; Dey, A. K. Stepwise formation of metal chelates of uranium (VI) and thorium (IV) with ammonium aurintricarboxylate. *J. Inorg. Nucl. Chem.* **1968**, *30*, 3134–3143.

(30) Avinashi, B. K.; Dwivedi, C. D.; Banerji, S. K. Potentiometric studies on chelate formation of ammonium aurintricarboxylate with bivalent copper. *J. Inorg. Nucl. Chem.* **1970**, *32*, 2641–2644.

(31) Can, M.; Sari, H.; Macit, M. Potentiometric study of the new synthesized 1-Benzyl-4-Piperazineglyoxime and 1-methyl-4-piperazineglyoxime and their divalent metal complexes. *Acta Chim. Slov.* **2003**, *50*, 1–14.

(32) Sari, H.; Can, M.; Macit, M. Potentiometric and Theoretical Studies of Stability Constants of Glyoxime Derivatives and their Nickel, Copper, Cobalt and Zinc Complexes. *Acta Chim. Slov.* **2005**, *52*, 317–322.

(33) Ogretir, C.; Duran, M.; Aydemir, S. Spectroscopic and Theoretical Study on Isomerism, Prototautomerism, and Acid Dissociation Constants of 2-Hydroxy-3-(3-oxo-1-phenylbutyl)chromen - 4-one. *J. Chem. Eng. Data* **2010**, *55*, 5634–6541.

(34) Ozkutuk, M.; Ogretir, C.; Arslan, T.; Kandemirli, F.; Koksoy, B. Acid Dissociation Constants of Some Novel Isatin Thiosemicarbazone Derivatives. *J. Chem. Eng. Data* **2010**, *55*, 2714–2718.

(35) Dewar, M. J. S.; Dieter, K. M. J. Evaluation of AM1 calculated proton affinities and deprotonation enthalpies. *J. Am. Chem. Soc.* **1986**, *108*, 8075–8086.

(36) Lajunen, L. H.; Portonova, R.; Piispanen Tolazzi, M. Stability constants for alpha- hydrocarboxylic acid complexes with protons and metal Ions and the accompanying enthalpy changes. Part I - Aromatic ortho-hydrocarboxylica acids. *Pure Appl. Chem.* **1997**, *69*, 329–381.

(37) Martell, A. E.; Smith, R. M. *Critical Stability Constants*; Plenum Press: New York, 1977; Vol. 3.

(38) Huheey, J. E.; Keiter, E. A.; Keiter, R. L. Inorganic Chemistry, Principles of Structure and Reactivity, Fourth ed., Harper Collins College Publishers. 1993.

(39) El-Gogary, T. M.; El-Bindary, A. A.; Hilali, A. S. Temperature and substituent effects on the dissociation constants of 5-azorhodanine derivatives. Semi-empirical quantum mechanical calculation. *Spectrochim. Acta, Part A.* **2002**, *58*, 447–455.

(40) Bebot-Bringaud, A.; Dange, C.; Fauconnier, N.; Gerard, C. Potentiometric and Spectrophotometric Studies of Phytic Acid Ionization and Complexation Properties Toward Co^{2+}, Ni^{2+}, Cu^{2+}, Zn^{2+} and Cd^{2+}. *J. Inorg. Biochem.* **1999**, *75*, 71–78.

(41) Al-Obaidi, F. N.; Sari, H.; Macit, M. Potentiometric study of the coordination tendency of 1, 2-Bis (4-benzylpiperidine)glyoxime toward some transition metal ions. *J. Chem. Eng. Data* **2010**, *55*, 5576–5580.

(42) Sharma, R. K.; Garg, B. S.; Kurosaki, H.; Goto, M.; Otsuka, M.; Yamamotoc, T.; Inoue, J. Aurintricarboxylic acid, a potent metal-chelating inhibitor of NFKB-DNA binding. *Bioorg. Med. Chem.* **2000**, *8*, 1819–1823.